Investigation of Fire Behavior of Rigid Polyurethane Foams Containing Fly Ash and Intumescent Flame Retardant by Using a Cone Calorimeter

Nazım Usta

Energy Division, Mechanical Engineering Department, Pamukkale University, Denizli 20070, Turkey

Received 11 February 2011; accepted 25 July 2011
DOI 10.1002/app.35352
Published online 21 November 2011 in Wiley Online Library (wileyonlinelibrary.com).

ABSTRACT: Cone calorimeter is one of the most useful bench-scale equipment which can simulate real-world fire conditions. Therefore, cone calorimeter tests have been the most important and widely used tests for research and development of fire behavior of polymeric materials. In this study, fire behavior of rigid polyurethane foams containing fly ash (up to 5 wt %) and intumescent flame retardant (up to 5 wt %) composed of ammonium polyphosphate/pentaerythritol was investigated by using a cone calorimeter. In addition, thermogravimetric analysis of the additives and the foams were also carried out to explain the effects of fly ash and intumescent flame retardant on fire behavior of the foams. Experimental results indicated that rigid polyurethane foam containing fly ash and the intumescent flame retardant in comparison with pure rigid polyurethane foam shows significantly enhanced fire resistance and thermal stability. © 2011 Wiley Periodicals, Inc. J Appl Polym Sci 124: 3372–3382, 2012

Key words: polyurethanes; flame retardance; calorimetry; fillers; intumescence

INTRODUCTION

Rigid polyurethane foams have been used in many industrial areas such as thermal insulation and automotive sectors due to their advantageous properties such as low thermal conductivity, low density, high abrasion resistance, good shock absorption. However, the rigid polyurethane foams are very combustible materials having fast flame spread and high heat release rates. Therefore, many studies have been performed for enhancing the fire behavior of rigid polyurethane foams.[1–10] In these studies, effects of different flame retardant materials, blowing agents and fillers have been investigated to produce fire resistive rigid polyurethane foams. Care should be taken regarding the compatibilities of flame retardants, blowing agents, and fillers with the raw materials of polyurethane foam and negative effects on the mechanical properties.

Levchik and Weil[11] presented a review about thermal decomposition, combustion, and fire-retardancy of polyurethanes. It was pointed out that thermal decomposition of polyurethanes usually starts at the thermally weakest links, which are allophanate and biuret, and it is followed by ureas, urethanes, and isocyanurate group. In addition, it was indicated that the burning of polyurethane foams proceeds in two stages. In the first stage, solid-phase burning may occur with the combustion of the isocyanate portion generating yellow smoke which may further decomposes to HCN and organic compounds. Nitrogen oxides are then formed by the conversion of a portion of the HCN. In the second stage, liquid pool burning may occur with the combustion of the polyol portion generating heat, CO, and CO_2. The flammability of the foams mainly depends on the structure of the polyol and the isocyanurate index. In addition, density of the foam and air flow over the foam are other very important factors for flame-spread. Furthermore, Weil and Levchik[12] prepared another review about commercial flame retardants. Flame-retardant materials may act either in the condensed phase or the vapor phase through a physical and/or chemical mechanism to hinder the combustion process during heating, pyrolysis, ignition, or flame spread.[13]

Recently, Singh and Jain[14] published a comprehensive review about the ignition, combustion, toxicity, and fire retardancy of rigid and flexible polyurethane foams. It was indicated that the fire retardancy of polyurethane can be achieved by using reactive, nonreactive (additive) and combination of reactive and nonreactive flame retardants. Although the reactive retardants join chemically into the foam, the nonreactive retardants are generally incorporated

Correspondence to: N. Usta (n_usta@pau.edu.tr or usta_n@yahoo.com).

Contract grant sponsor: The Scientific and Technological Research Council of Turkey (TUBITAK); contract grant number: 108T246.

Contract grant sponsor: State Planning Organization of Turkey (DPT); contract grant number: 2003K120950.

into the foam by physical means and do not take part in the foaming reaction.

The reactive flame retardants which are mainly based on phosphorus and halogen slow down decomposition of the foam and maintain the fire retardancy.[15–18] Since the halogenated flame retardants generate dangerous toxic gases and heavy smoke during combustion, halogen-free flame retardants have been under consideration for fire resistance of polyurethane foams. Phosphorus- and nitrogen-based materials forming char layer and reducing the evolution of toxic smokes have been mainly preferred.[19]

The nonreactive flame retardants based on phosphorus, carbon, halogens, aluminum, sulfur, nitrogen, boron, antimony, and silicones retain a degree of fire retardancy on a weight basis. If they are compatible with the foam, they take action as plasticizers; if not, they are considered as fillers. The addition of fillers mainly decreases the amount of raw materials resulting in reduction in the concentration of decomposition gases.[13,20] A synergistic effects may be generated with the combination of reactive and nonreactive flame retardants.[21,22]

Although an adequate fire resistance can be generally obtained with high loading of metal hydroxides, which is typically more than 60 phr,[11,23–25] the high loading may result in negative effects on the mechanical properties.[26,27] The negative effects were explained with insufficient interactions between the polymer and the metal hydroxides.[23] Therefore, studies have been focused on intumescent flame retardants which usually composed of a char forming agent, a catalyst for char formation and a foaming agent.[24] The foams which contain intumescent flame retardants swell when exposed to fire or heat to form a carbonaceous mass acting as a barrier to heat, air, and pyrolysis product.[13,28] Flame retardancy of ammonium polyphosphate,[29–34] expandable graphite,[28,33–40] and melamine compounds[24,41] as intumescent flame retardants for polyurethane foams were investigated by many researchers. In addition, Meng et al.[34] studied the effects of expandable graphite (EG) and ammonium polyphosphate (APP) on the flame retardancy and mechanical properties of the rigid polyurethane foam.

Fly ash, a by-product of coal-fired power station, may be defined as an inorganic material which may be mainly composed of SiO_2, Al_2O_3, Fe_2O_3, CaO, SO_3, MgO, Na_2O, K_2O, MnO, TiO_2, and P_2O_5. The chemical composition of fly ash may vary depending on the type of coal and combustion used in the station.[42] Although fly ash is used in different industrial applications such as construction industry; most of fly ash is stored in lagoons adjacent to power stations and causes environmental pollution. Therefore, researchers try to find new methods to use fly ash in new applications based on the chemical composition of fly ash. In this concept, some studies related to the usage of fly ash in polymeric material productions were performed. Soyama et al.[43] investigated that fly ash addition into polycarbonate significantly improves the flame retardancy. Fire proof panels were formed by simple compaction or the vacuum filtration using fly ash, waste paper and other industrial wastes.[44,45] Gu et al.[46] studied on epoxy resin filled with fly ash to obtain a promising advanced low density composite material. Rama and Rai[47] studied mechanical properties of pure epoxy and hydroxyl-terminated polyurethane elastomer toughened epoxy composites filled with fly ash. In addition, fly ash was used as a filler in high-density polyethylene to develop lightweight reinforced composites.[48] Wu et al.[49] performed a study on the preparation and dynamic mechanical properties of polyurethane-modified epoxy composites filled with functionalized fly ash particulates.

Fly ash was used as a flame-retardant material in production of polymer matrix composite particleboard from pistachio shells[50] and urea-formaldehyde-based particleboard from hazelnut shells.[51] The improvement in fire resistance of the particleboards was explained with the inert characteristic of fly ash at fire. The effects of fly ash, nanosize and commercial $CaCO_3$ additions on mechanical and thermal properties of polybutadiene rubber[52–54] and ethylene–propylene–diene rubber[55] were investigated. In general, it was mentioned that the particle size, the amount of the fillers, the chemical composition and the uniform dispersion of particles in the rubber matrix are very important for the improvement in all the properties. In addition, it was pointed out that the inorganic fillers promote formation of the char layer acting as a good insulator and mass transfer barrier, which slows down the escape of the volatile products and improves the burning resistance of the material.

In an earlier work performed under the ongoing project, the rigid polyurethane foams containing up to 5.0 wt % fly ash, composed of mainly silica and alumina, and 5.0 wt % intumescent flame retardant including ammonium polyphosphate (APP) and pentaerythritol (PER) were successfully produced using an industrial polyurethane injection machine.[56] The effects of the intumescent flame retardant and fly ash filler on the physicomechanical properties of PUR foams were investigated. It was found that 5 wt % fly ash and 5.0 wt % intumescent flame retardant addition enhanced physicomechanical properties of PUR. Although the flammability tests of PUR foam samples performed according to UL 94 standard[57] showed that flame resistance of PUR foam was improved with the addition of the fly ash and the intumescent flame retardant, the test did not give detailed information about the fire behavior. Hence, the fire behavior of rigid polyurethane foams containing fly ash and intumescent flame retardant still needs to be investigated.

Cone calorimeter tests have been the most important and widely used tests for the research and development of fire behavior of polymeric materials.[58,59] In addition, the cone calorimeter is one of the most useful bench-scale equipment attempting to simulate real-world fire conditions.[60] The cone calorimeter tests can generate quantitative analysis to materials flammability research by investigating parameters such as time to ignition (TTI), heat release rate (HRR), total heat released (THR), residual mass, smoke, and CO/CO_2 release rates.[61]

This work is the complementary of the previous work[56] which was performed in behalf of the same project. It investigates the fire behavior of rigid polyurethane foams containing fly ash and intumescent flame retardant by using a cone calorimeter. Cone calorimeter tests were conducted on the PUR foams with and without the fly ash/the intumescent flame retardant. Thermogravimetric (TG) analysis of the additives and the foams were also studied to explain the effects of the fly ash and the intumescent flame retardant on fire behavior of the foam.

EXPERIMENTAL

Materials

Raw materials consisting of Elastopor H2011/4 as a polyol component containing all necessary additives for the foaming process and PMDI 92140 polymeric diphenylmethane diisocyanate as an isocyanate component were purchased from Elastogran BASF Group in industrial grade. The density and viscosity of the polyol at 25°C are 1130 kg/m^3 and 240 mPas, respectively. Meanwhile, the density and viscosity of the isocyanate at 25°C are 1230 kg/m^3 and 210 mPas, respectively, and NCO content of the isocyanate is 31.2%.[62] Fly ash of Kemerkoy Power Station (Mugla–Turkey) fuelled with lignite was used in the experiments. The fly ash referred to as FA in the paper is mainly composed of CaO (35.26%), SiO_2 (26.25%), SO_3 (14.8%), Al_2O_3 (12.72), Fe_2O_3 (7.04%), and MgO (2.11%). The crystal modification ammonium polyphosphate (APP, Exolit AP 423, $n > 1000$) kindly supplied from Clariant–Turkey was phase II. The average particle size (d_{50}) was $\sim$ 8 μm. Pentaerythritol (PER) kindly supplied by MKS Marmara Chemistry Company has particle size below 75 μm.

Sample preparation

A laboratory scale PUR foam injection machine designed and produced by Cersan Machine (İstanbul, Turkey) was used to obtain the PUR foams with and without the fly ash and the intumescent flame retardant. The working principle of the machine is same as that of the industrial PUR foam injection machine. However, it has smaller tanks and pumps. Therefore it may be used easily in the laboratory. The proportion of the isocyanate/polyol was adjusted as 1.18/1 in the machine. The amounts of components were adjusted to obtain the PUR foams with the density of 40 ± 0.5 kg/m^3. The fine FA particles which were obtained by sieving below 25 μm were used as the filler in PUR foams. The FA concentration was varied from 1.0 wt % to 5.0 wt % in 1 wt % increment. The FA concentration could not be increased over 5 wt % due to sedimentation of fly ash particles in the tank of the injection machine. An intumescent flame retardant containing ammonium polyphosphate (APP) as an acid source/blowing agent and pentaerythritol (PER) as a carbonific agent was used in the experiments. Although the different mass ratios of APP and PER were used in preparation of the intumescent flame retardant, the best mass ratio in terms of fire behavior was found to be the mass ratio of 2/1 (APP/PER). Similar result was found by Demir et al.[63] for polypropylene. This combination of the intumescent flame retardant is referred to as IFR in the paper. The loadings of IFR were 2.5 wt % and 5.0 wt % of total weight of the raw materials. In addition, IFR loading of 5.0 wt % was introduced to the PUR foam containing 5.0 wt % FA. The loading of IFR could not be increased in polyurethane production using the injection machine due to the increase in viscosity of the mixture of polyol, FA and IFR.[56] Heidolph Silent Crusher M Model homogenizer which is a rotor-stator type of mechanical homogenizers with a speed range up to 26,000 rpm was used to disperse IFR and FA into the polyol component.

The mixture obtained with the machine was poured into preheated aluminum molds which were put under a heated press to keep the temperature at 40 ± 2°C for 30 min. After completing the curing process under the press, the samples were removed from the molds and put in a conditioning device for complete curing at the temperature 23 ± 1°C and relative humidity 50 ± 3% for 24 h. All samples were cut at the size of 100 ± 0.5 mm × 100 ± 0.5 mm × 50 ± 0.5 mm for cone calorimeter tests.

In the article, only test results of PUR, PUR containing 5 wt % FA (PUR/FA), PUR containing 5 wt % IFR (PUR/IFR), PUR containing 5 wt % FA and 5 wt % IFR (PUR/FA/IFR) are given for the sake of clarity. PUR, PUR/FA, PUR/IFR, and PUR/FA/IFR abbreviations are used in the rest of the paper. The main formulations of these foams are listed in Table I.

TG analysis

Perkin–Elmer Diamond thermogravimetric analysis (TG/DTA) equipment was used to perform thermal gravimetric analysis of APP, PER, FA, PUR foam samples between 40 and 800°C at a rate of 20°C/

TABLE I
Formulations of PUR, PUR/FA, PUR/IFR, and PUR/FA/IFR

	H2011/4 Polyol component(g)	PMDI 92140 Isocyanate component (g)	FA (g)	IFR (g)
PUR	45.9 ± 0.1	54.1 ± 0.1	0	0
PUR/FA	43.6 ± 0.1	51.4 ± 0.1	5 ± 0.1	0
PUR/IFR	45.9 ± 0.1	54.1 ± 0.1	0	5 ± 0.1
PUR/FA/IFR	43.6 ± 0.1	51.4 ± 0.1	5 ± 0.1	5 ± 0.1

min under nitrogen. Ceramic pans were used in the experiments. The real time weight loss and derivative weight loss were recorded via special software during the experiment. For all thermogravimetric analyses, the mean of three replicate measurements was reported for each sample.

Cone calorimeter

The cone calorimeter manufactured according to ASTM E-1354[64] and ISO-5660[65] standards by Vega Automation Company (Denizli, Turkey) was used to investigate the fire behavior of PUR foams with and without FA/IFR. The cone calorimeter uses a ring sampler and a gas sampling apparatus composed of a pump, filters, a cold trap and a by-pass system as it is advised in the standards.[64,65] The apparatus also includes a multi component Siemens Ultramat 23 system with NDIR (Nondispersive Infrared) technology for carbon monoxide (CO), carbon dioxide (CO_2), and nitrogen oxide (NO) measurements, and a Siemens Oxymat 6 which measures oxygen (O_2) using paramagnetic alternating pressure method. A heated line was used between the ring sampler and the gas sampling apparatus to avoid condensation. The calibrations and tests were performed according to the standard procedures. Each specimen of the size of 100 mm × 100 mm × 50 mm was wrapped in aluminum foil and exposed horizontally to an external heat flux of 35 ± 1 kW/m^2 which corresponds to a common heat flux in mild fire scenario.[66] All measurements related to mass loss, temperatures, smoke production, O_2, CO, CO_2, and NO evolutions were recorded simultaneously via special software in 1 s increment. HRR (heat release rate), TTI (time to ignition), PHRR (peak heat release rate), FPI (fire performance index–TTI/PHRR), AHRR (average heat release rate) and THR (total heat released) values were determined from the measurements. HRR values (kW/m^2) were calculated from the standard equations given in ASTM E-1354[64] and ISO-5660[65] standards as follows:

$$\mathrm{HRR}\ (t) = \frac{1}{A_s}.\frac{\Delta h_c}{r_o}.(1.1).C\sqrt{\frac{\Delta P}{T_e}}.\frac{X^0_{O_2} - X_{O_2}(t)}{(1.105) - (1.5).X_{O_2}(t)} \quad (1)$$

where "t" is the time, "A_s" is the initially exposed area of the sample (m^2), "Δh_c" is the net heat of combustion (kJ/kg), "r_o " is the stoichiometric oxygen/fuel mass ratio, "1.1" is the ratio of the oxygen to air molecular weights, "C" is the calibration constant (m$^{1/2}$ kg$^{1/2}$ K$^{1/2}$), "ΔP" is the orifice meter pressure differential (Pa), "T_e" is the absolute temperature of gas at the orifice meter (K), X^0_{O2} is the average of the oxygen analyzer output measured during the 1-min baseline measurements and X_{O_2} is the oxygen analyzer reading. During the experiment, after removing the radiation shield continuous spark ignition was provided and the TTI (s) was recorded for each specimen which ignites. The PHRR is the maximum value of a HRR curve. FPI (m^2.s/kW) was calculated by dividing TTI to PHRR[67–69]:

$$\mathrm{FPI} = \frac{\mathrm{TTI}}{\mathrm{PHRR}} \quad (2)$$

Meanwhile, THR (MJ/m^2) was calculated by the integration of heat release rate for the measurement time:

$$\mathrm{THR} = \int_a^b \mathrm{HRR}(t).dt \quad (3)$$

where "a" is the time after the last negative heat release rate reading occurring at the beginning of the test, "b" is the final reading recorded for the test. In addition, AHRR (kW/m^2) was calculated by using the following equation:

$$\mathrm{AHRR} = \frac{\int_c^d \mathrm{HRR}(t).dt}{\Delta t} \quad (4)$$

where "c" is the time after the last negative heat release rate reading occurring at the beginning of the test, "d" is the time reading for the desired average value and "Δt" is the time interval (d-c). In this study, the trapezium rule was used to calculate the integrated values as advised in ISO-5660[65] standard. The cone calorimeter parameters given in this study were average of three replicated experiments for

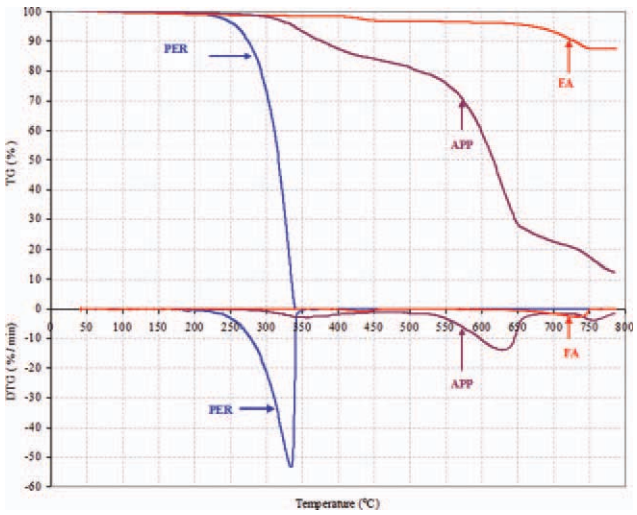

Figure 1 Thermogravimetric analysis of APP, PER, and FA. [Color figure can be viewed in the online issue, which is available at wileyonlinelibrary.com.]

each sample and the parameters were reproducible to within ±5% which is acceptable value for the standards.[64,65]

Microscopy

An optical Nikon SMZ 1500 Stereo microscope connected a personal computer was used to examine the morphology of the samples. The optical images were taken from different areas of each sample and the mean diameter of the cells were calculated according to ASTM D3576-04.[70]

RESULTS AND DISCUSSION

TG analysis

Thermal degradation studies are strongly related to investigating fire behavior of materials. Therefore, thermogravimetric analyses of the additives and the foams were initially performed. The TG and DTG curves of APP, PER and FA are shown in Figure 1 and the results obtained by TG and DTG analysis are given Table II. The results include the temperatures at 5, 10, and 50% weight losses ($T_{5\ wt\ \%}$, $T_{10\ wt\ \%}$, and $T_{50\ wt\ \%}$), the maximum degradation temperatures in first, second and third stage (T_{1max}, T_{2max}, and T_{3max}), the maximum rates of degradation in first, second and third stage (R_{1max}, R_{2max}, and R_{3max}) and the residues at 785°C. It can be seen that there exists a great difference in the thermal decomposition of APP, PER, and FA. PER began to decompose at about 175°C and had only one decomposition process in which the maximum degradation temperature (T_{1max}) and the maximum rate of degradation (R_{1max}) were 334.9°C and 53.3%/min, respectively, whereas APP began to decompose at about 250°C and had three decomposition processes between 40°C and 785°C. $T_{5\ wt\ \%}$, $T_{10\ wt\ \%}$, and $T_{50\ wt\ \%}$ of PER were determined as 258.6°C, 275.1°C, and 317.4°C, respectively. Meanwhile, $T_{5\ wt\ \%}$, $T_{10\ wt\ \%}$, and $T_{50\ wt\ \%}$ of APP were found to be 338.5°C, 368.4°C, and 616.2°C, respectively. PER decomposed completely at about 345°C while the residual weight of APP was about 12% at 785°C. The evolution products in the first process of APP are mainly ammonia and water, and crosslinked polyphosphoric acids are formed simultaneously[58,71] and T_{1max} and R_{1max} were 359.1°C and 3.1%/min, respectively. The second process occurred in the range of 500–700°C, which is the main decomposition process of APP and the polyphosphoric acids may be evaporated and/or dehydrated to phosphorus oxides,[71] and the weight loss was about 78%.[58] In this process, T_{2max} and R_{2max} were determined as 629.1°C and 14.1%/min, respectively. The third decomposition occurred in the range of 725–775°C and T_{3max} and R_{3max} were 758.6°C and 3.9%/min, respectively. In the fly ash analysis, two decomposition processes occurred. In the first process, T_{1max} and R_{1max} were 436.7°C and 0.9%/min. Moreover, in the second process, T_{2max} and R_{2max} were 734.3°C and 2.8%/min, respectively. $T_{5\ wt\ \%}$ and $T_{10\ wt\ \%}$ of FA were determined as 669.7°C and 728.9°C, respectively, and FA lost only about 12 wt % between 40°C and 785°C.

Figure 2 shows the TG and DTG curves of the pure PUR, PUR/FA, PUR/IFR, and PUR/FA/IFR composites. In addition, the results obtained by TG and DTG analysis are given Table III. The weight loss for all foams started at about 100°C with evolving water and continued with the dissociation of the

TABLE II
Results Obtained by TG and DTG Analysis For APP, PER, and FA

	$T_{5\ wt\ \%}$ (°C)	$T_{10\ wt\ \%}$ (°C)	$T_{50\ wt\ \%}$ (°C)	T_{1max} (°C) R_{1max} (%/min)	T_{2max} (°C) R_{2max} (%/min)	T_{3max} (°C) R_{3max} (%/min)	Residue at 785°C (wt %)
APP	338.5 ± 1	368.4 ± 1	616.2 ± 1	359.1 ± 1 3.1 ± 0.2	629.1 ± 1 14.1 ± 0.2	758.6 ± 1 3.9 ± 0.2	12.24 ± 0.3
PER	258.6 ± 1	275.1 ± 1	317.4 ± 1	334.9 ± 1 53.3 ± 0.5	–	–	0
FA	669.7 ± 1	728.9 ± 1	–	436.7 ± 1 0.9 ± 0.1	734.3 ± 1 2.8 ± 0.1	–	87.4 ± 0.4

$T_{5\ wt\ \%}$, $T_{10\ wt\ \%}$, and $T_{50\ wt\ \%}$ represent temperatures at 5, 10, and 50% weight loss, respectively.
T_{1max}, T_{2max}, and T_{3max} represent maximum degradation temperatures in first, second and third stage, respectively.
R_{1max}, R_{2max}, and R_{3max} represent maximum rate of degradation in first, second and third stage, respectively.

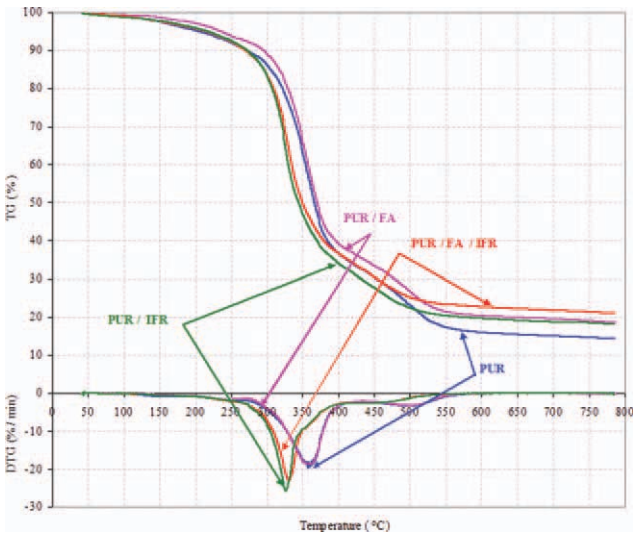

Figure 2 Thermogravimetric analysis of PUR, PUR/FA, PUR/IFR, and PUR/FA/IFR. [Color figure can be viewed in the online issue, which is available at wileyonlinelibrary.com.]

thermally weakest links which are allophanate and biuret.[11] Despite PUR and PUR/FA exhibited similar three decomposition processes; the FA addition resulted in slight delays in the decomposition processes of PUR and more residues at high temperatures. The first decomposition process of PUR took place at 248.5°C (T_{1max}) with R_{1max} of 1.9%/min. The second process was the main decomposition process, and T_{2max} and R_{2max} values were 357.4°C and 19.9%/min, respectively. The third process occurred at about 501.4°C with R_{1max} of 3.4%/min. The maximum degradation temperatures of PUR/FA were 0.3–3.8°C higher than those of PUR and the maximum rates of degradation of PUR/FA were 0.1–1.2%/min lower than those of PUR. Although $T_{5\ wt\ \%}$, $T_{10\ wt\ \%}$, and $T_{50\ wt\ \%}$ of PUR were 205.6, 272.0, and 366.2°C, respectively, the corresponding temperatures for PUR/FA were 235.9, 295.3, and 369.8°C, respectively. Moreover, it should be pointed out that the residue of PU/FA (18.6 wt %) was higher than that of PUR (14.4 wt %) at 785°C.

The IFR addition into the PUR and PUR/FA accelerated the decomposition processes[11,72] and PUR/IFR and PUR/FA/IFR composites decomposed early in comparison with PUR and PUR/FA. The reason for an early decomposition of PUR/IFR and PUR/FA/IFR is due to the intumescent flame retardant addition. IFR decomposes and produces a char layer which can partially hinder the decomposition of the material.[11,58,72] The first decomposition processes of PUR/IFR and PUR/FA/IFR, which were not significant as those of PUR and PUR/FA, occurred at about 150°C with fairly small of the maximum rates of degradation. Similar to PUR and PUR/FA, the second process was the main decomposition process for both PUR/IFR and PUR/FA/IFR, T_{2max} and R_{2max} values for them were 326.7°C and 25.7%/min, and 331.8°C and 22.9%/min, respectively. The third decomposition of PUR/IFR and PUR/FA/IFR occurred at around 450.4°C (T_{3max}) with R_{3max} of 2.6%/min and 454.4°C (T_{3max}) and R_{3max} of 2.7%/min, respectively. In addition, $T_{5\ wt\ \%}$, $T_{10\ wt\ \%}$, and $T_{50\ wt\ \%}$ of PUR/IFR were 217.6, 272.3, and 343.9°C, respectively, and the corresponding temperatures for PUR/FA/IFR were 214.7, 269.8, and 349.8°C, respectively. Although the residue of PUR/IFR was 18.0% at 785°C, the maximum high temperature residue (20.9%) was achieved with PUR/FA/IFR foam.

Cone calorimeter tests

The HRR, PHRR, TTI, THR, and FPI are important parameters in cone calorimeter tests to compare different materials and to express the intensity of a fire. The HRR and the THR curves of the PUR, PUR/FA, PUR/IFR, and PUR/FA/IFR materials with respect to time at a heat flux of 35 kW/m^2 are shown in Figures 3 and 4, respectively. The results obtained from the figures are given in Table IV. All samples revealed similar characteristics of thermally thick charring (residue forming) samples in which an initial increase in HRR appears until an efficient char layer is formed and then the char layer thickens resulting in a decrease in HRR.[73] However, PUR burned very fast after ignition and the HRR of PUR reached to the peak value of 132.7 kW/m^2. Meanwhile, significant reductions in the HRR values and

TABLE III
Results Obtained by TG and DTG Analysis For PUR, PUR/FA, PUR/IFR, and PUR/FA/IFR

Sample codes	$T_{5\ wt\ \%}$ (°C)	$T_{10\ wt\ \%}$ (°C)	$T_{50\ wt\ \%}$ (°C)	T_{1max} (°C) R_{1max} (%/min)	T_{2max} (°C) R_{2max} (%/min)	T_{3max} (°C) R_{3max} (%/min)	Residue at 785 °C (wt %)
PUR	205.6 ± 1	272.0 ± 1	366.2 ± 1	248.5 ± 1 1.9 ± 0.1	357.4 ± 1 19.9 ± 0.2	501.4 ± 1 3.4 ± 0.2	14.4 ± 0.3
PUR/FA	235.9 ± 1	295.3 ± 1	369.8 ± 1	248.8 ± 1 1.8 ± 0.1	361.2 ± 1 18.7 ± 0.2	502.4 ± 1 3.2 ± 0.2	18.6 ± 0.3
PUR/IFR	217.6 ± 1	272.3 ± 1	343.9 ± 1	153.0 ± 1 0.8 ± 0.1	326.7 ± 1 25.7 ± 0.2	450.4 ± 1 2.6 ± 0.2	18.0 ± 0.3
PUR/FA/IFR	214.7 ± 1	269.8 ± 1	349.8 ± 1	155.5 ± 1 0.9 ± 0.1	331.8 ± 1 22.9 ± 0.2	454.4 ± 1 2.7 ± 0.2	20.9 ± 0.3

$T_{5\ wt\ \%}$, $T_{10\ wt\ \%}$, and $T_{50\ wt\ \%}$ represent temperatures at 5, 10, and 50% weight loss, respectively.
T_{1max}, T_{2max}, and T_{3max} represent maximum degradation temperatures in first, second, and third stage, respectively.
R_{1max}, R_{2max}, and R_{3max} represent maximum rate of degradation in first, second, and third stage, respectively.

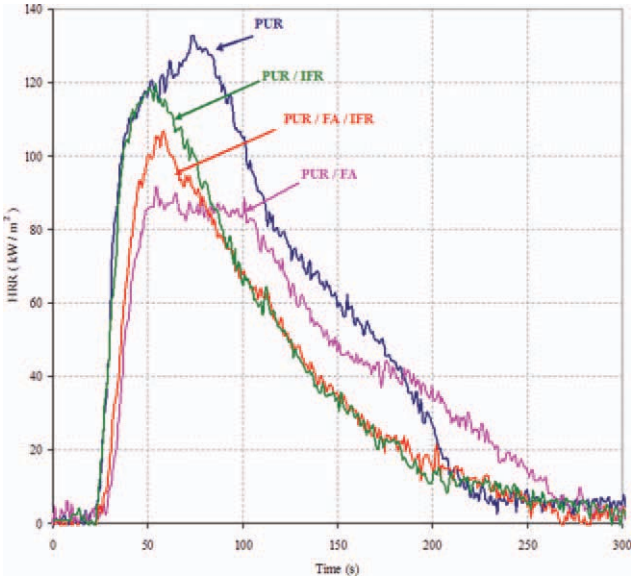

Figure 3 The heat release rates (HRR) of PUR, PUR/FA, PUR/IFR, and PUR/FA/IFR. [Color figure can be viewed in the online issue, which is available at wileyonlinelibrary.com.]

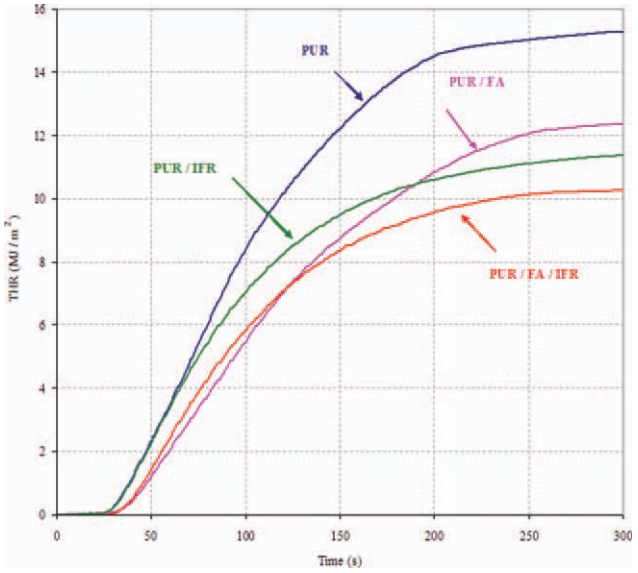

Figure 4 The total heat released (THR) values of PUR, PUR/FA, PUR/IFR, and PUR/FA/IFR. [Color figure can be viewed in the online issue, which is available at wileyonlinelibrary.com.]

peak HRR (PHRR) were achieved with FA, IFR, and FA/IFR additions to PUR. It should be mentioned that PHRR is an important parameter which can indicate the intensity of fires.[61] Furthermore, the HRR curve of PUR/FA represented a plateau after an initial increase. This plateau remained nearly constant for ~ 50 s before decreasing of HRR. This kind of plateau did not appear in PUR/IFR and PUR/FA/IFR. Also, the increase in HRR of PUR/IFR occurred more quickly than PUR/FA. This situation may be explained with the early decomposition of IFR which was mentioned above. Although the PHRR values of PUR/IFR (119.6 kW/m^2) and PUR/FA/IFR (106.8 kW/m^2) were higher than that of PUR/FA (91.7 kW/m^2), later on the HRR values of them decreased quickly and were lower than that of PUR/FA during the rest of the time.

The THR values of the samples shown in Figure 4 up to a burn time of 300 s could help to clarify the effects of FA and IFR additions into PUR.[73,74] Obviously FA, IFR, and IFR/FA additions decreased the THR of PUR. Although PUR/IFR and PUR/FA/IFR generated more heat with respect to PUR/FA up to approximately 190 s and 125 s, respectively, the heat generation reduced with the char formation on the material mainly due to the IFR. As it is known that the char layer can partially prevent the heat transfer and flame spread. This in turn protects the underlying material from further burning.[58] In other words, it can be said that the presence of IFR and FA/IFR in PUR decreased the HRR values strongly when compared to PUR and PUR/FA. Although the THR of PUR/FA (12.36 MJ/m^2) is ~ 19% less than that of PUR (15.29 MJ/m^2), the incorporation of IFR and FA/IFR into PUR resulted in ~ 26 and 33% reduction in the THR as 11.35 MJ/m^2 and 10.24 MJ/m^2, respectively.

Meanwhile time to ignition (TTI) value was increased with the addition of IFR and FA/IFR. Although the TTI values of PUR and PUR/FA were ~ 19 s, the PUR containing IFR and FA/IFR were more resistant to ignition with the TTI values ~ 21 s and 24 s, respectively. As it is well known that the longer ignition time is desired for a material.[75] In

TABLE IV
Cone Calorimeter Results of PUR, PUR/FA, PUR/IFR, and PUR/FA/IFR

Sample Codes	TTI (s)	PHRR (kW/m^2)	FPI (m^2 s/kW)	AHRR (at 180 s) (kW/m^2)	THR (for 300 s) (MJ/m^2)	Residue (wt %)
PUR	19 ± 1	132.7 ± 5	0.1432 ± 0.0093	76.78 ± 2.4	15.29 ± 0.5	39.1 ± 0.8
PUR/FA	19 ± 1	91.7 ± 4	0.2072 ± 0.0142	55.9 ± 2.8	12.36 ± 0.5	39.6 ± 0.6
PUR/IFR	21 ± 1	119.6 ± 5	0.1756 ± 0.0111	57.1 ± 2.2	11.35 ± 0.4	41.8 ± 0.6
PUR/FA/IFR	24 ± 1	106.8 ± 4	0.2247 ± 0.0126	50.9 ± 2.5	10.24 ± 0.4	47.0 ± 0.5

TTI, time to ignition; PHRR, peak heat release rate; FPI, fire performance (propagation) index; AHRR, average heat release rate; THR, total heat released.

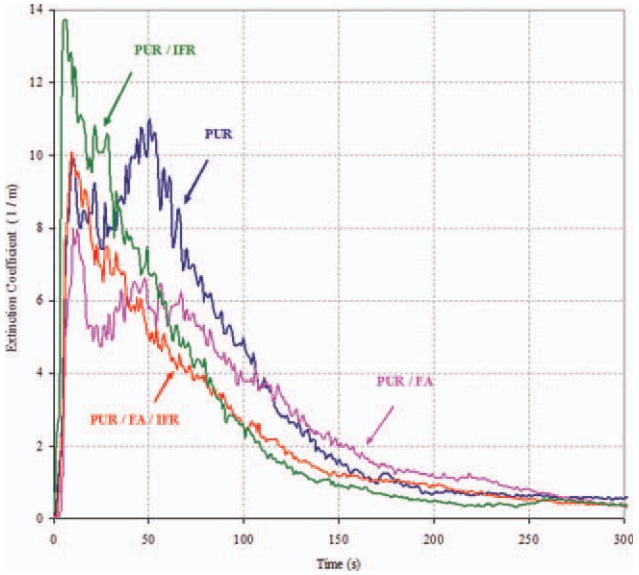

Figure 5 The extinction coefficients of PUR, PUR/FA, PUR/IFR, and PUR/FA/IFR. [Color figure can be viewed in the online issue, which is available at wileyonlinelibrary.com.]

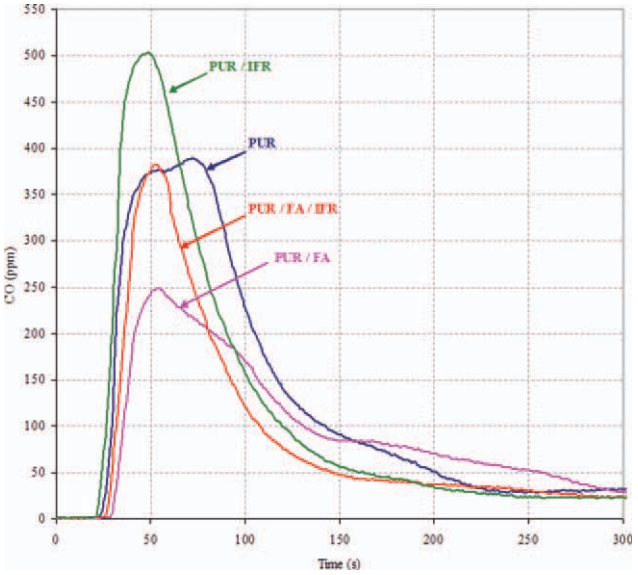

Figure 6 The CO emissions of PUR, PUR/FA, PUR/IFR, and PUR/FA/IFR. [Color figure can be viewed in the online issue, which is available at wileyonlinelibrary.com.]

addition, FPI values also indicate the safety rank of the materials. The higher the FPI means the higher the safety rank of the materials.[67–69] As it is shown in Table IV that FA and IFR addition into the PUR resulted in increasing of FPI values. Although the detailed results of FA additions (1–5 wt %) were not given in the paper, it should be pointed out that as the concentration of FA was increased in the foam, the fire resistance of the foam was increased in terms of FPI. The highest FPI value was obtained with the addition of FA/IFR.

Smoke and CO which are considered as the major cause of poisoning during fires are measured in cone calorimeter tests.[75] Smoke and CO productions in combustion of materials strongly depend on fire and material properties. During the combustion of PUR foams, the carbon initially is converted into gas carbon oxides, total hydrocarbon, and soot.[76] Both smoke and CO productions are generated due to incomplete combustion of the foam. Figure 5 shows the extinction coefficients representing smoke emissions of the samples while Figure 6 shows CO emissions. The smoke and CO trends are very similar. FA addition (PUR/FA) decreased the peak values of smoke and CO. This may be explained with the reduction of the combustible material content in the foam and fuel lean condition in certain periods. The smoke and CO generations of PUR/FA were greater than those of PUR after 115 and 160 s, respectively. This may imply that although there were small smoke and CO peaks, but the reaction of the foam extended more than that of PUR. However, IFR addition (PUR/IFR) initially resulted in increasing of smoke and CO, but later on the smoke and CO values sharply decreased below PUR after 35 s, and PUR/FA after 60 s. This may be explained by the intumescent effect. The IFR decomposes quickly and then generate char layer which prevents the linkage of heat from the materials.[14] The addition of FA and

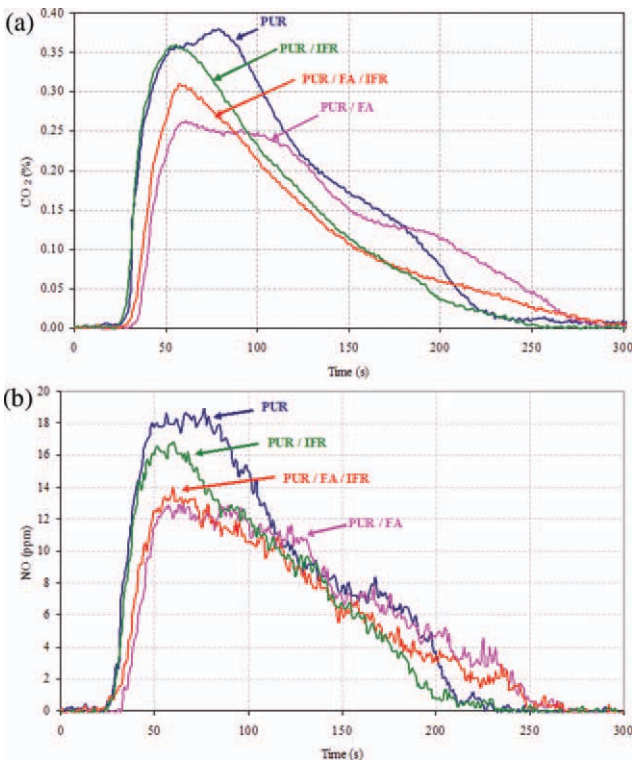

Figure 7 The CO_2 (a) and NO (b) emissions of PUR, PUR/FA, PUR/IFR, and PUR/FA/IFR. [Color figure can be viewed in the online issue, which is available at wileyonlinelibrary.com.]

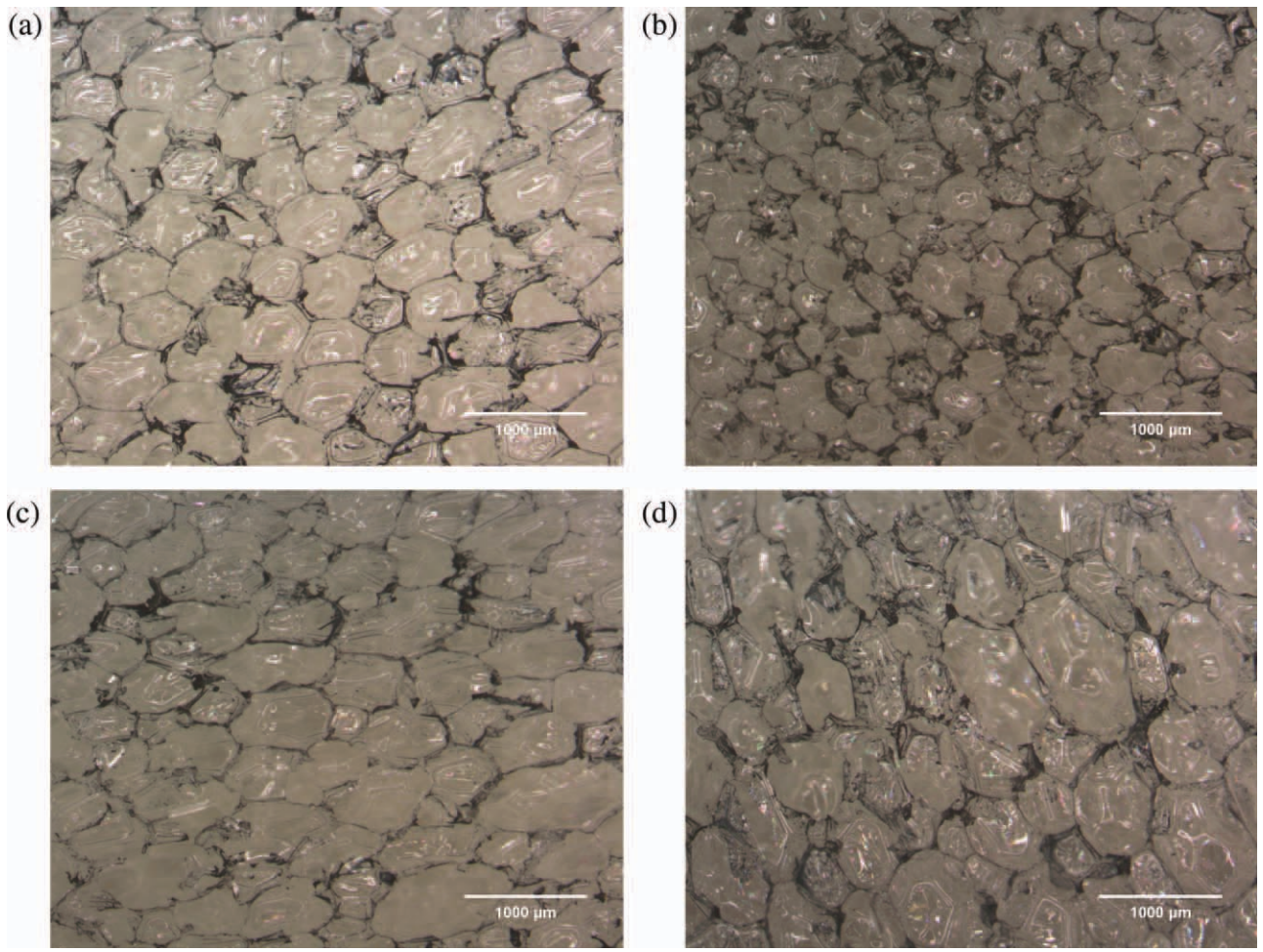

Figure 8 The optical microscopy pictures of (a) PUR, (b) PUR/FA, (c) PUR/IFR, and (d) PUR/FA/IFR foams. [Color figure can be viewed in the online issue, which is available at wileyonlinelibrary.com.]

IFR together (PUR/FA/IFR) showed the best performance in terms of CO and smoke emissions. Although PUR/FA/IFR initially generated more smoke and CO with respect to the FA addition, it resulted in less smoke and CO in the rest of the time. In addition, it should be pointed out that although HRR decreased to nearly zero at the end of the burn time of 300 s, there were still some smoke and CO emissions because of the smoldering combustion of the materials.[77] Although the smoldering combustion is fairly important for rigid polyurethane materials, it can be said that it did not play a significant role in the present study conditions.

The CO_2 and NO emissions are shown in Figure 7. It is clear that CO_2 emissions of PUR/FA, PUR/IFR and PUR/FA/IFR composites were lower than that of PUR. The CO_2 emissions of the foams showed similar trends with the HRR curves, as expected.[76] Since the combustible material of PUR/FA was less than that of PUR, the CO_2 emissions of PUR/FA were less than that of PUR. Although the peak values of PUR/IFR and PUR/FA/IFR were higher than that of PUR/FA, the CO_2 emissions of them decreased quickly due to char formation generated by IFR.[71] Because the char layer protected the underlying material from further burning.[58]

In general, NO emission is not measured in cone calorimeter tests. However, it was measured in the present experiments due to the fact that low level of NO emissions is fairly dangerous. Valencia et al.[76] reported that nitrogen gas species (HCN, NH_3, N_2O, NO_2), except NO, were absent or present in quantities less than 2 ppm in gas products generated during combustion of polyether polyurethane foam at different irradiance levels. The formation of NO emission can be explained with two reasons. One is the high temperature resulted during combustion and the other is the nitrogen in the materials. The lower HRR values of the composite foams may imply the lower temperature in the combustion of the composite foams resulting lower NO. Since polyurethanes contain nitrogen in their structure,[76] they can produce HCN during pyrolysis or combustion. Nitrogen oxides are then formed by the conversion of a portion of the HCN.[11] The decreasing of peak NO emission in PUR/FA may be attributed to the

decreasing the polyurethane content of the foam composite and the lower HRR. The peak NO emission of PUR/IFR was slightly lower than that of PUR due to lower HRR, but it was higher than that of PUR/FA. This may imply that the NO generation may be mainly affected with the nitrogen content in the foam. This may be supported with the result of PUR/FA/IFR which was very close to that of PUR/FA.

The char structure may elucidate the combustion behavior of composites. It is known that the efficient char formation prevents the heat transfer between the burning substrate and the flame zone, which protects the underlying materials from further burning. Furthermore, it can retard the pyrolysis of polymers.[24] The residues left after the cone calorimeter tests were examined to elucidate effects of FA and IFR additions on the combustion. The residual masses of the samples are given in Table IV. Although the residue of PUR was 39.1 ± 0.8 wt %, FA, and IFR additions resulted in increasing of the residual mass as 39.6 ± 0.6 wt % and 41.8 ± 0.6 wt %, respectively. Meanwhile, FA/IFR additions gave the largest residue with ~ 47.0 ± 0.5 wt %. Although efficient intumescent char could not be formed from the burning of the PUR/FA/IFR, its residual mass value was ~ 20% higher than that of PUR. This may be explained with the synergistic effects of FA and IFR.[78]

Cell structure

Figure 8 shows the optical microscopy pictures of the cross-sectional surfaces of PUR, PUR/FA, PUR/IFR, and PUR/FA/IFR foams. The shape of cells in PUR was approximately polyhedron and the average equivalent cell diameter was calculated as 783 ± 72 μm. However, the addition of FA, IFR, and FA/IFR into PUR slightly changed the shapes of the cells. The average equivalent cell diameters of PUR/FA, PUR/IFR, and PUR/FA/IFR were 608 ± 57 μm, 768 ± 121μm, and 854 ± 103 μm, respectively. The decrease in the cell size of PUR/FA may be attributed to the nucleation of FA during the foam preparation.[20,79] In other words, it means that FA particles acted as nucleating agents during the formation of PUR/FA.[80] Furthermore, it should be pointed out that the thermal conductivity of PUR/FA (25.4 mW/mK) with small cell size was slightly lower than that of PUR (26.6 mW/mK).[56,81] Meanwhile the thermal conductivies of PUR/IFR and PUR/FA/IFR were 26.6 mW/mK and 27.1 mW/mK, respectively. Although the closed cell contents of the foams were not measured, it was assumed that there were no significant changes in the closed cell contents of the foams which could affect the thermal conductivity values.[79]

CONCLUSIONS

The fire behavior of PUR containing FA, IFR, and FA/IFR was investigated using the cone calorimeter tests. Significant reductions in the HRR and the PHRR values were achieved with FA, IFR, and FA/IFR additions to PUR. Although the THR of PUR/FA (12.36 MJ/m^2) was approximately 19% less than that of PUR (15.29 MJ/m^2), the incorporation of IFR and FA/IFR into PUR resulted in approximately 26 and 33% reductions in the THR, respectively. Meanwhile, the addition of the FA, IFR and FA/IFR into the PUR led to decreases in smoke, CO, CO_2 and NO emissions. Although FA addition resulted in slight increase in the residual mass, IFR and FA/IFR additions led to more residual masses. As a result, it can be said that PUR/FA/IFR gave the best performance among the foams in terms of fire resistive. This means that IFR had a good synergistic effect with FA in the PUR/FA/IFR composite foams.

References

1. Brzozowski, B. K.; Pietruszka, N.; Gajewski, J.; Stankiewicz, R. Polimery (Warsaw) 1998, 43, 252.
2. Tang, Z.; Maroto-Valer, M. M.; Andresen, J. M.; Miller, J. W.; Listemann, M. L.; McDaniel, P. L.; Morita, D. K.; Furlan, W. R. Polymer 2002, 43, 6471.
3. Pielichowski, K.; Kulesza, K.; Pearce, E. M. J Polym Eng 2002, 22, 195.
4. Czuprynski, B.; Paciorek-Sadowska, J.; Liszkowska, J. Polimery (Warsaw) 2002, 47, 727.
5. Czuprynski, B.; Liszkowska, J.; Paciorek-Sadowska, J. Polimery (Warsaw) 2004, 49, 187.
6. Wang, J. Q.; Chow, W. K. J Appl Polym Sci 2005, 97, 366.
7. Modesti, M.; Zanella, L.; Lorenzetti, A.; Bertani, R.; Gleria, M. Polym Degrad Stab 2005, 87, 287.
8. Kulesza, K.; Pielichowski, K.; German, K. J Anal Appl Pyrolysis 2006, 76, 243.
9. Singh, B.; Gupta, M.; Tarannum, H. J Biobased Mater Bioenergy 2010, 4, 397.
10. Paciorek-Sadowska, J; Czuprynski, B.; Liszkowska, J.; Jaskolowski, W. Polimery (Warsaw) 2010, 55, 99.
11. Levchik, S. V.; Weil, E. D. Polym Int 2004, 53, 1585.
12. Weil, E. D.; Levchik, S. V. J Fire Sci 2004, 22, 183.
13. Lu, S. Y.; Hamerton, I. Prog Polym Sci 2002, 27, 1661.
14. Singh, H.; Jain, A. K. J Appl Polym Sci 2009, 111, 1115.
15. Tashev, E.; Zabski, L.; Shenkov, S.; Borissov, G. Eur Polym Mater 1992, 28, 689.
16. Modesti, M.; Simioni, F. Cell Polym 1994, 13, 277.
17. Prociak, A.; Pielichowski, J.; Modesti, M.; Simioni, F. Cell Polym 1997, 16, 284.
18. Prociak, A.; Pielichowski, J.; Modesti, M.; Simioni, F.; Checchin, M. Polimery (Warsaw) 2001, 46, 692.
19. Singh, H.; Jain, A. K.; Sharma, T. P. J Appl Polym Sci 2008, 109, 2718.
20. Thirumal, M.; Khastgir, D.; Singha, N. K.; Manjunath, B. S.; Naik, Y. P. J Macromol Sci Part A-Pure Appl Chem 2009, 46, 704.
21. Zatorski, W.; Brzozowski, Z. K.; Kolbrecki, A. Polym Degrad Stab 2008, 93, 2071.
22. Bastin, B.; Paleja, R.; Lefebvre, J. J Cell Plast 2003, 39, 323.
23. Thirumal, M.; Singha, N. K.; Khastgir, D.; Manjunath, B. S.; Naik, Y. P. J Appl Polym Sci 2010, 116, 2260.

24. Lv, P.; Wang, Z.; Hu, K.; Fan, W. Polym Degrad Stab 2005, 90, 523.
25. Zhang, J.; Wang, X.; Zhang, F.; Horrocks, A. R. Polym Test 2004, 23, 225.
26. Bahattab, M. A.; Mosnacek, J.; Basfar, A. A.; Shukri T. M. Polym Bull 2010, 64, 569.
27. Liu, S. M.; Huang, J. Y.; Jiang, Z. J.; Zhang, C.; Zhao, J. Q.; Chen, J. J Appl Polym Sci 2010, 117, 3370.
28. Bian, X. C.; Tang, J. H.; Li, Z. M. J Appl Polym Sci 2008, 109, 1935.
29. Modesti, M.; Lorenzetti, A. Polym Degrad Stab 2002, 78, 341.
30. Wang, J. C.; Chen, Y. H. J Fire Sci 2005, 23, 55.
31. Ni, J. X.; Song, L.; Hu, Y. A.; Zhang, P.; Xing, W. Y. Polym Adv Technol 2009, 20, 999.
32. Ni, J. X.; Tai, Q. L.; Lu, H. D.; Hu, Y. A.; Song, L. Polym Adv Technol 2010, 21, 392.
33. Barikani, M.; Askari, F.; Barmar, M. Cell Polym 2010, 29, 343.
34. Meng, X. Y.; Ye, L.; Zhang, X. G.; Tang, P. M.; Tang, J. H.; Ji, X.; Li, Z. M. J Appl Polym Sci 2009, 114, 853.
35. Shi, L.; Li, Z. M.; Xie, B. H.; Wang, J. H.; Tian, C. R.; Yang, M. B. Polym Int 2006, 55, 862.
36. Bian, X. C.; Tang, J. H.; Li, Z. M.; Lu, Z. Y.; Lu, A. J Appl Polym Sci 2007, 104, 3347.
37. Thirumal, M.; Singha, N. K.; Khastgir, D.; Manjunath, B. S.; Naik, Y. P. J Appl Polym Sci 2008, 110, 2586.
38. Ye, L.; Meng, X. Y.; Ji, X.; Li, Z. M.; Tang, J. H. Polym Degrad Stab 2009, 94, 971.
39. Modesti, M.; Lorenzetti, A.; Simioni, F.; Camino, G. Polym Degrad Stab 2002, 77, 195.
40. Shi, L.; Li, Z. M.; Yang, M. B.; Yin, B.; Zhou, Q. M.; Tian, C. R.; Wang, J. H. Polym Plast Technol Eng 2005, 44, 1323.
41. Thirumal, M.; Khastgir, D.; Nando, G. B.; Naik, Y. P.; Singha, N. K. Polym Degrad Stab 2010, 95, 1138.
42. Chaipanich, A.; Nochaiya, T.; Wongkeo, W.; Torkittikul, P. Mater Sci Eng A 2010, 527, 1063.
43. Soyama, M.; Inoue, K.; Iji, M. Polym Adv Technol 2007, 18, 386.
44. Vilches, L. F.; Fernandez-Pereira, C.; Olivares del Valle, J.; Rodríguez-Pinero, M. A.; Vale, J. J Chem Technol Biotechnol 2002, 77, 361.
45. Vilches, L. F.; Fernández-Pereira, C.; Olivares del Valle, J.; Vale, J. Chem Eng J 2003, 95, 155.
46. Gu, J.; Wu, G.; Zhang, Q. Mater Sci Eng A 2007, 452–453, 614.
47. Rama, S. R.; Rai, S. K. J Compos Mater 2009, 43, 3231.
48. Deepthi, M. V.; Sharma, M.; Sailaja, R. R. N.; Anantha, P.; Sampathkumaran, P.; Seetharamu, S. Mater Des 2010, 31, 2051.
49. Wu, G.; Gu, J.; Zhao, X. J Appl Polym Sci 2007, 105, 1118.
50. Guru, M.; Sahin, M.; Tekeli, S.; Tokgoz, H. High Temp Mater Process 2009, 28, 3, 191.
51. Guru, M.; Aruntas, Y.; Tuzun, F. N.; Bilici, I. Fire Mater 2009, 33, 413.
52. Mishra, S.; Sonawane, S. H.; Badgujar, N.; Gurav, K.; Patil, D. J Appl Polym Sci 2005, 96, 6.
53. Mishra, S.; Shimpi, N. G. Polym Plast Technol Eng 2008, 47, 72.
54. Shimpi, N. G.; Mishra, S. J Nanopart Res 2010, 2, 2093.
55. Mishra, S.; Patil, U. D.; Shimpi, N. G. Polym Plast Technol Eng 2009, 48, 1078.
56. Tarakcilar, A. R. J Appl Polym Sci 2011, 120, 2095.
57. UL 94 Standard, Test for flammability of plastic materials for parts in devices and appliances. Northbrook, IL: Underwriters Laboratories Inc., 1996.
58. Wu, K.; Wang, Z.; Hu, Y. Polym Adv Technol 2008, 19, 1118.
59. Beyer, G. J Fire Sci 2007, 25, 65.
60. Morgan, A. B.; Bundy, M. Fire Mater 2007, 31, 257.
61. Chung, Y.; Kim Y.; Kim S. J Ind Eng Chem 2009, 15, 888.
62. BASF The Chem Company. Technical data sheet for Elastofoam I 4501/109 and Iso PMDI 92040 2005.
63. Demir, H.; Arkis, E.; Balkose, D.; Ulku, S. Polym Degrad Stab 2005, 89, 478.
64. ASTM E 1354. Standard Test Method for Heat and Visible Smoke Release Rates for Materials Using an Oxygen Consumption Calorimeter, ASTM International, West Conshohocken, PA, U.S.A. 2004.
65. ISO 5660. Reaction-to-fire tests e heat release, smoke production and mass loss rate. Geneva, Switzerland: ISO; 2002.
66. Bourbigot, S.; Samyn, F.; Turf, T.; Duquesne, S. Polym Degrad Stab 2010, 95, 320.
67. Gallina, G.; Bravin, E.; Badalucco, C.; Audisio, G.; Armanini, M.; De Chirico, A.; Provasoli, F. Fire Mater 1998, 22, 15.
68. He, S.; Hu, Y.; Song, L.; Tang, Y. J Fire Sci 2007, 25, 109.
69. Wang, L.; Wu, X.; Wu, C.; Yu, J.; Wang, G.; Jiang P. J Appl Polym Sci 2011, 121, 68.
70. ASTM D3576-04, Standard Test Method for Cell Size of Rigid Cellular Plastics. ASTM International, West Conshohocken, PA, U.S.A., 2004.
71. Duquesne, S.; Le Bras, M.; Bourbigot, S.; Delobel, R.; Poutch, F.; Camino, G.; Eling, B.; Lindsay, C.; Roels, T. J Fire Sci 2000, 18, 456.
72. Duquesne, S.; Le Bras, M.; Bourbigot, S.; Delobel, R.; Camino, G.; Eling, B.; Lindsay, C.; Roels, T.; Vezin, H. J Appl Polym Sci 2001, 82, 3262.
73. Schartel, B.; Hull, T. R. Fire Mater 2007, 31, 327.
74. König, A.; Fehrenbacher, U.; Kroke, E.; Hirth, T. J Fire Sci 2009, 27, 187.
75. Checchin, M.; Cecchini, C.; Cellarosi, B.; Sam, F.O. Polym Degrad Stab 1999, 64, 573.
76. Valencia, L. B.; Rogaume, T.; Guillaume, E.; Rein, G.; Torero, J. L. Fire Saf J 2009, 44, 933.
77. Price, D.; Liu, Y.; Hull, T. R.; Milnes, G. J.; Kandola, B. K.; Horrocks, A. R. Polym Int 2000, 49, 1153.
78. Levchik, S. V. In Flame Retardant Polymer Nanocomposites, Morgan, A.B., Wilkie, C. A., Eds.; Wiley: New Jersey, 2007; Chapter 1.
79. Kang, J. W.; Kim, J. M.; Kim, M. S.; Kim, Y. H.; Kim, W. N. Macromol Res 2009, 17, 856.
80. Modesti, M.; Lorenzetti, A.; Besco, S. Polym Eng Sci 2007, 47, 1351.
81. Kim, S. H.; Lee, M. C.; Kim, H. D.; Park, H. C.; Jeong, H. M.; Yoon, K. S.; Kim, B. K. J Appl Polym Sci 2010, 117, 1992.